Program Digest, 2019 IEEE International Ultrasonics Symposium (IUS)
Glasgow, Scotland, October 6-9, 2019

Diffraction-limited spatial resolution using synthetic focus time-of-flight ultrasound tomography

Michael Jaeger
Institute of Applied Physics
University of Bern
Bern, Switzerland
michael.jaeger@iap.unibe.ch

Tobias Schweizer
Institute of Applied Physics
University of Bern
Bern, Switzerland

Cyril Etter
Institute of Applied Physics
University of Bern
Bern, Switzerland

Patrick Stähli
Institute of Applied Physics
University of Bern
Bern, Switzerland
patrick.staehli@iap.unibe.ch

Martin Frenz
Institute of Applied Physics
University of Bern
Bern, Switzerland
martin.frenz@iap.unibe.ch

***Abstract*— Ultrasound tomography (UT) reconstructs an image of speed-of-sound (SoS) based on analysing ultrasound (US) transmitted through tissue from a variety of angles. In ray tomography (RT), the time-of-flight (ToF) of US is related to integrals of SoS along acoustic rays. It is perceived that, while allowing a numerically efficient reconstruction, RT has the disadvantage of low spatial resolution and geometric distortions due to diffraction and refraction. We propose a modification to RT where, for each angle, the detected signal is synthetically backpropagated into the tissue sample and the ToF is analysed in a spatially resolved way, resulting in a 2D (for planar systems) map of ToF values. These maps are then accumulated and ramp-filtered as in FBP to obtain the SoS. We demonstrate in simulations and in phantoms that this technique inherently reduces the influence of the wave nature of US propagation on the final SoS image, allowing diffraction-limited resolution without the need for a computationally expensive full-wave inversion.**

Keywords—speed of sound, breast imaging, migration, filtered backprojection

I. Introduction

Ultrasound tomography (UT) reconstructs an image of speed-of-sound (SoS) and attenuation based on analysing ultrasound (US) transmitted through tissue from a variety of angles. *In vivo* results of imaging the female breast demonstrate the potential of UT for differentiating between benign and malignant tumour types. The various different implementations of UT can be grouped into three main categories:

Ray tomography (RT). In its most simple form, UT is based on the ray approximation of sound propagation, linking the detected time-of-flight (ToF) of ultrasound (US) through the breast to line integrals of slowness (inverse of SoS) [1]. Assuming straight propagation paths, the spatial distribution of the slowness can then be reconstructed from the ToF values, e.g. using the linear and thus computationally cheap filtered back-projection [2], or by solving a linear equation system [3, 4]. Refraction can be accounted for by permitting bent rays requiring a more expensive nonlinear reconstruction [5, 6]. It is perceived that RT cannot account for diffraction, resulting in a spatial resolution on the order of $\sqrt{L\lambda}$ (L: ray length, λ: wavelength) [7, 8], far worse than the theoretical diffraction limit given by λ. A further difficulty in RT has been the need for ToF picking. First arrival detection is typically used together with the Eikonal forward solver for bent-ray reconstruction, but the definition of the first arrival is not straight forward.

Diffraction tomography (DT). Based on the 1st order Born approximation, the tissue's acoustic properties can be reconstructed directly from the detected signals as opposed to the ToF, either in the frequency domain [9] or using a linear superposition of Greens functions [10]. Due to its linearity, this technique is again computationally efficient and in principle allows a diffraction-limited resolution. It is, however, only applicable if the phase distortion of US waves (relative to a reference SoS) are below π, a condition that is not fulfilled in the breast [9]. To solve this problem, RT can be used to derive a first guess of the reference SoS on which the calculation of the Greens functions is based [10].

Full-wave inversion (FWI). In this approach, the reconstruction is based on iteratively solving the wave equation, given the measurements, for the acoustic properties by optimising a data fidelity function. FWI thus accounts for both refraction and diffraction, and provides unprecedented high diffraction-limited resolution quantitative SoS images of the breast [11]. On the downside, each iteration requires the simulation of the acoustic wavefield for a number of frequencies and for all or a subset of the transmitting elements. This makes FWI computationally expensive, especially when aiming at a 3D reconstruction. Apart from that, FWI can be trapped in local minima of the fidelity function due to phase distortions above π. One way to ensure a global minimum is achieved is by stepping from low frequencies where the $< \pi$ condition is fulfilled, to high frequencies that provide high spatial resolution [12][11]. This approach is only feasible if permitted by the transducer bandwidth. A different or additional way to avoid local minima and – in addition – reduce computational cost, is again to combine FWI with a first guess derived from RT [12].

In this paper we show that ToF-based UT can achieve diffraction-limited spatial resolution and geometric accuracy similar to FWI or DT but with the computational efficiency of RT, without the need for bent-ray modelling. This is achieved by introducing a signal back-migration step prior to ToF determination, which synthetically focuses the data in a dynamic way along "ray paths" so that the ray approximation underlying RT is fulfilled to a large extent (synthetic-focus ray tomography, SF-RT).

II. THEORY

For the following, consider the 2D tomographic setup depicted in Fig. 1a, where a linear single-element transmitter launches plane waves into the sample volume, and a linear array receiver detects the through-transmitted wave field. For full tomographic coverage, the transducer pair is rotated around the sample by >180° while acquiring signals at specific angles.

To develop SF-RT we depart from identifying the main problem of RT: due to diffraction and refraction, sound propagation deviates from the assumed straight and thin (on the order of λ) ray paths, so that the detected ToF cannot be related to straight line integrals of SoS. At a location $\boldsymbol{r}$ of interaction of the wavefield with the tissue's SoS, however, local variations of SoS are imprinted on the wavefield *with the spatial resolution of* λ. In the perspective of DT, the wavefield including an interaction at point $\boldsymbol{r}$ can be written as a superposition of the scattered field from this interaction, with the wavefield that would be present excluding this interaction. It is the spatial separation between $\boldsymbol{r}$ and a location of detection $\boldsymbol{r}'$ that causes the spatial spreading of the scattered field and thus the information on the interaction.

To retrieve the spatial resolution at the location of interaction, the spatial spreading must be reverted. The first step in SF-RT is therefore to (synthetically) focus all scattered fields to the points $\boldsymbol{r}$ from where they emerge, by migrating the detected wavefield back into the sample. This can be done either in the time- or in the frequency domain. In time domain, synthetically focused signals $\hat{s}(\boldsymbol{r}, t)$ are generated from the signals $s(\boldsymbol{r}'_n, t)$ detected on elements n using a delay-and-sum algorithm:

$$\hat{s}(\boldsymbol{r}, t) = \sum_{n=1}^{N} s\big(\boldsymbol{r}'_n, t + \hat{t}(\boldsymbol{r}, \boldsymbol{r}'_n)\big) \tag{1}$$

Thereby $\hat{t}(\boldsymbol{r}, \boldsymbol{r}'_n)$ is the anticipated time of propagation from $\boldsymbol{r}$ to $\boldsymbol{r}'_n$, assuming an *a priori* estimation of SoS. Fig. 1b illustrates how the back-migration influences the ToF profile of a pulsed plane wave after propagating though a circular area with elevated SoS relative to a uniform background (simulation). This result demonstrates that, while the ToF profile at the detecting aperture is "blurred" in relation to the SoS contrast area, the ToF at the depth of the contrast area follows the profile that one would expect from straight-ray propagation.

The first basic hypothesis behind SF-RT is therefore that back-migration allows to detect ToF profiles that indeed follow the straight-ray assumption, thus a diffraction-limited resolution SoS reconstruction becomes possible using RT.

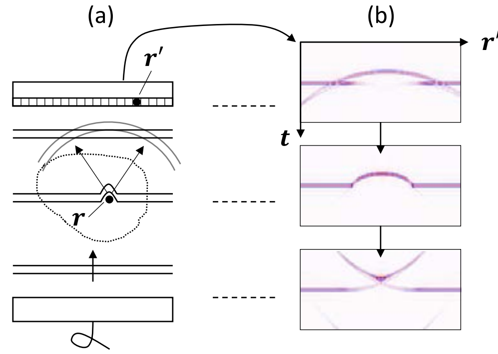

Fig. 1. a) 2D tomographic setup with a linear element transmitting plane waves into the sample, and a linear array receiver detecting the scattered wavefield. b) Illustration of back-migration of the detected signal, at the depths indicated by dashed lines.

Back-migration does not allow to focus to all locations of interaction simultaneously. The reason is seen in Fig. 1b: the imprint of the contrast area on the migrated signals is defocused not only towards the receiving aperture, but also towards the transmitter. Therefore, the imprint of SoS variations located at different depths are focused only at those specific depths, thus at each depth, the ToF profile of the back-migrated field is always a combination of defocused and focused parts. To take this into account, we generate not only one ToF profile per angle, but a 2D matrix of ToF values corresponding to a 2D plane of points $\boldsymbol{r}$ to which the signals are back-migrated. In total for all angles, this results in a 3D matrix instead of the conventional 2D sinogram.

For SoS reconstruction, we use a modified FBP that accounts for this type of data. In the conventional FBP, for each angle, a 1D vector of ToF values is backprojected onto a 2D matrix as illustrated in Fig. 2a, and the matrices from all angles are summed after a transformation from measurement to lab coordinates. Instead, we sum the 2D ToF maps after coordinate transformation (Fig. 2b). In the modified FBP, the backprojection step *after* ToF determination is thus replaced by a back-migration *before* ToF determination. The final step, the application of the ramp filter in the spatial frequency domain, is the same as in the conventional FBP.

It is the second fundamental hypothesis of SF-RT that – using this modified FBP – diffraction-limited resolution is obtained in all $\boldsymbol{r}$ even though their imprint on the ToF profiles is – for each angle – only focused at one back-migration depth.

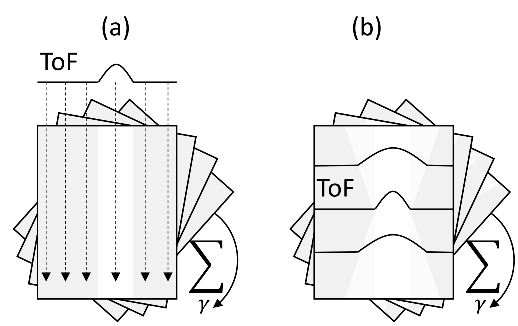

Fig. 2. a) Conventional FBP, where the 1D ToF profiles are backprojected along the assumed straight rays of sound propagation, and summed over all angles. b) In the modified FBP, the 2D ToF maps are summed over all angles.

This hypothesis is based on following model of the influence of a SoS variation in a small region around a point $\boldsymbol{r}''$ on the ToF values $\tau(\boldsymbol{r},\gamma)$: first we split the slowness distribution (inverse of SoS) $\sigma(\boldsymbol{r})$ into a background slowness σ_b and the spatial profile of the excess slowness $\Delta\sigma$ describing the variation.

$$\sigma(\boldsymbol{r}) = \sigma_b(\boldsymbol{r}) + \Delta\sigma(\boldsymbol{r}) \quad (2)$$

Then we make the fundamental assumption that the ToF map $\tau(\boldsymbol{r},\gamma)$ can accordingly be written as the sum of a background ToF τ_b and the ToF difference $\Delta\tau$ imprinted by $\Delta\sigma$ (this is a more general form of the assumption of linearity in RT).

$$\tau(\boldsymbol{r},\gamma) = \tau_b(\boldsymbol{r},\gamma) + \Delta\tau(\boldsymbol{r}'',\boldsymbol{r},\gamma) \quad (3)$$

Fig. 3 illustrates the spatial distribution of $\Delta\tau$ for two different γ for a single circular contrast region. The important observation is that, no matter how defocused the back-migrated field is outside the contrast area, *at* the contrast area it leads to a *sharp* ToF profile perpendicular to the main propagation axis for *all* angles. Therefore the 2D ToF maps are locally identical to a straight-ray backprojection, and the FBP should lead to a correct reconstruction of $\Delta\sigma$. Thereby we implicitly assumed that back-migration takes σ_b into account, so that τ_b is known and $\Delta\tau$ can be determined. Starting from a uniform reference medium with *a priori* slowness σ_b, $\Delta\tau$ is measured relative to this reference (e.g. water). Assuming that the linearity still holds for the full sample, the deviation $\Delta\sigma$ from the reference of the full sample can be reconstructed from $\Delta\tau$.

The next point of attention is the ToF picking. In any point the signal typically consists of a sequence of pulses from different "propagation paths" – due to diffraction and refraction – that connect the transmitter to the respective point. First arrival detection is often used in RT to pic the ToF of the first of these pulses. We use a different approach where we define an average $\Delta\tau$ of all pulses, corresponding to the average influence of SoS along the different paths. For this purpose we correlate the Fourier transform of a signal $\hat{s}(\boldsymbol{r},t)$, $\tilde{s}(\boldsymbol{r},\omega)$, with its reference $\tilde{s}_{ref}(\boldsymbol{r},\omega)$ measured at the same position. If the signals are shifted copies of each other (* indicates conjugate):

$$C(\boldsymbol{r},\omega) = \tilde{s}_{ref}(\boldsymbol{r},\omega)\cdot\tilde{s}(\boldsymbol{r},\omega)^* = \left|\tilde{s}_{ref}\right|^2 exp(\Delta\tau\cdot\omega) \quad (4)$$

The $\Delta\tau$ can in principle be derived from the phase angle of C, however, $\Delta\tau$ can be larger than half the wavelength of the lowest available ω, resulting in phase aliasing. Therefore we use instead:

$$T(\omega) = C(\omega)C(\omega+\Delta\omega)^* = |\ldots|^2 exp(\Delta\tau\cdot\Delta\omega) \quad (5)$$

so that $\Delta\tau$ can be determined from the phase angle of T without aliasing if $\Delta\omega$ is appropriately chosen. As said, signals are normally not perfect shifted copies of the reference. Therefore the average of (5) over the available ω is used so that the phase angle represents an average $\Delta\tau$.

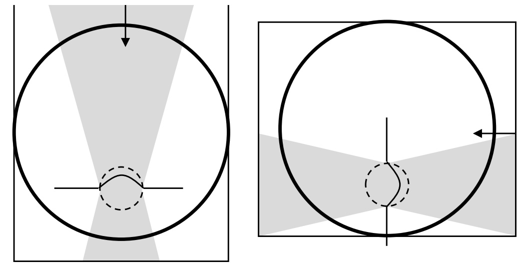

Fig. 3. Illustration of the spatial distribution of the ToF imprint (grey) of a circular contrast region (dashed circle) inside the sample volume (solid circle), for two different detection angles (main propagation axis indicated by arrow).

Because $\Delta\tau$ is determined in the frequency domain, it is practical to perform back-migration directly in the frequency domain instead of time domain:

$$\tilde{s}(\boldsymbol{r},\omega) = \sum_{n=1}^{N}\tilde{s}(\boldsymbol{r}'_n,\omega)\cdot exp\left(\mathrm{i}\omega\hat{t}(\boldsymbol{r},\boldsymbol{r}'_n)\right) \quad (6)$$

III. Materials and Methods

We built an experimental lab-top UT system according to the geometry shown in Fig. 1a, inspired by e.g. the system of QT Ultrasound labs [11]. For transmission, an Accuscan Paintbrush A342S-SU (5 MHz centre frequency, 51 mm aperture length) (Olympus) is used. For reception, an ATL L7-4 clinical array probe (5 MHz centre frequency, 38.4 mm aperture length) is used in conjunction with a Verasonics V1-64. The transducers are coupled through acoustic windows to opposing sides of a water tank. The tank can be translated in the horizontal plane to increase the aperture length, and rotated for acquiring a 2D tomographic data set. Phantoms were built from gelatin, agar, and oil-in-gelatin emulsions, to provide a nonuniform spatial distribution of SoS with a realistic contrast of breast tissue.

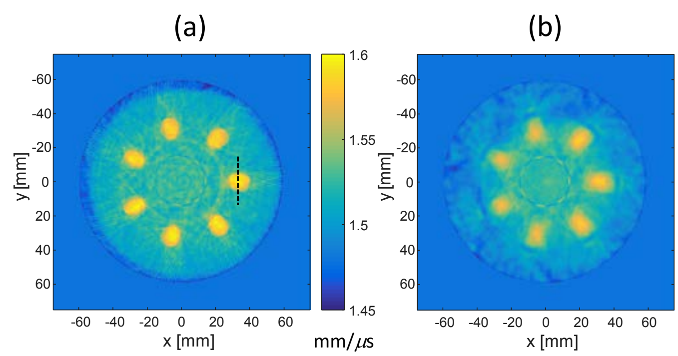

Fig. 4. a) SoS image of phantom containing circular inclusions with positive SoS contrast inside uniform background, using back-migration in conjunction with the modified FBP. b) SoS image without back-migration and using the conventional FBP.

IV. Results

Fig. 4a shows the SoS image of a simple phantom where cylindrical inclusions with positive SoS contrast were embedded inside a uniform background. The circular shape of the inclusions is nicely reproduced. Also note the excellent uniformity of the phantom's background material as well as the circular phantom-water interface. In comparison, the SoS image when determining ToF without back-migration and using conventional FBP (Fig. 4b) shows a markedly degraded resolution, non-uniform SoS in the background, and the phantom boundary is missing.

Fig. 5a shows the image (using SF-RT) of a cylindrical breast phantom that contained an outer "fat" layer with negative SoS contrast relative to an inner "glandular" part. The water-fat and fat-gland interfaces are nicely resolved, and the lumens reconstructed with excellent uniformity. In Fig. 5b, the glandular part contained 4 inclusions, 2 with negative and 2 with positive contrast. In comparison to Fig. 4a, these inclusions are less well resolved. This is explained by a violation of the linearity condition: the wavefield that probes the inclusions is refracted twice at the irregular fat-gland interface, leading to multiple intersecting propagation paths and thus to an ambiguity in ToF between line integral and average ToF of different paths. Further improvement of the image is thus possible by reducing the number of possible paths, by synthetic transmit focusing (Fig. 5c). Note that, in comparison, the conventional FBP fails at reconstructing boundaries and inclusions (Fig. 5d).

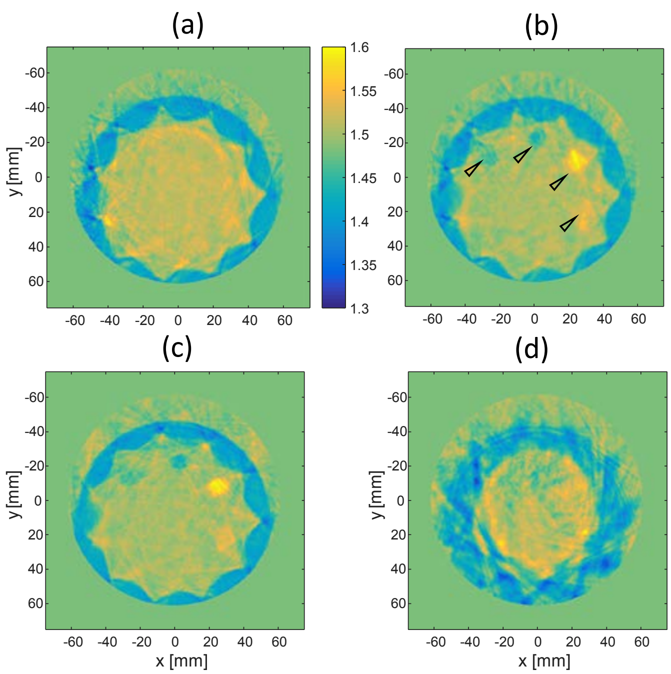

Fig. 5. a) SoS image of breast phantom. b) Same phantom but with 4 inclusions located in the imaging plane (arrowheads). c) Influence of synthetic transmit focusing. d) Conventional FBP result.

V. Discussion

We would like to point out that the markedly improved performance of SF-RT in comparison to conventional RT was achieved by combing concepts from RT, DT and FWI in an efficient way: when performing the back-migration in the frequency domain, SF-RT is similar to a DT reconstruction in the sense that (6) can be regarded as a superposition of Green's functions, but with two important differences: (i) instead of the field amplitude, the phase of the wavefield (corresponding to $\Delta\tau$) is used to derive the SoS, akin at the Rytov instead of the Born approximation; (ii) instead of analyzing one ω at a time, the comparison of wave fields at different ω is used, to avoid aliasing. Going a step further, instead of using (6) for back-migration of the frequency components, a Fourier split-step/ hybrid angular spectrum technique (parabolic approximation to the Helmholtz equation) [13] can be used. Then, the back-migration step is an analogue to the 1st application of the Jacobian in FWI [14]. Again, the differences to FWI are the same as mentioned above. Even though our approach may not compare with state-of-the art FWI results in terms of contrast resolution, we foresee that it has important applications for a quasi-real time display of SoS (e.g. for data integrity checks) and for an optimum starting guess to improve the accuracy of DT or reduce the computational cost of FWI. Similar to FWI, SF-RT may be employed in an iterative way, and we foresee that the convergence rate may be substantially faster.

Acknowledgment

This project has received funding from the European Union's Horizon 2020 research and innovation programme H2020 ICT 2016-2017 under grant agreement No 732411 and is an initiative of the Photonics Public Private Partnership. It is supported by the Swiss State Secretariat for Education, Research and Innovation (SERI) under contract number 16.0162. The opinions expressed and arguments employed herein do not necessarily reflect the official view of the Swiss Government.

References

[1] G. Zografos, et al., "Novel technology of multimodal ultrasound tomography detects breast lesions " Eur Radiol 23, 2013, pp. 673-683
[2] J.R. Jago and T.A. Whittingham, "Experimental studies in transmission ultrasound computed tomography " Phys Med Biol, 36(11), 1991, pp. 1515-1527
[3] N. Duric and P. Littrup, "Detection of breast cancer with ultrasound tomography: first results with the computed ultrasound risk evaluation (CURE) prototype " Med Phys 34(2), 2007, pp. 773-785
[4] J.F. Greenleaf and R.C. Bahn, "Clinical imaging with transmissive ultrasonic computerized tomography," IEEE Biomed Eng, BME-28(2), 1981, pp. 177-185
[5] C. Li, N. Duric, P. Littrup, and L. Huang, "In vivo breast sound-speed imaging with ultrasound tomography," Ult Med Biol, 35(10), 2009, pp. 1615-1628
[6] S. Li, et al., "Refraction corrected transmission ultrasound computed tomography for application in breast imaging," Med Phys, 37(5), 2010, pp. 2233-2246
[7] P.R. Williamson, "A guide to the limits of resolution imposed by scattering in ray tomography," Geophysics 56(2), 1991, pp. 168-323
[8] G.T. Schuster, "Resolution limits for crosswell migration and traveltime tomography," Geophysical Journal International, 127(2), 1996, pp. 427-440
[9] F. Simonetti, L. Huang, N. Duric, and P. Littrup, "Diffraction and coherence in breast ultrasound tomography: a study with a toroidal array " Med Phys, 36(7), 2009, pp. 2955-2965
[10] P. Huthwaite and F. Simonetti, "High-resolution imaging without iteration: a fast and robust method for breast ultrasound tomography," J Acoust Soc Am, 130(3), 2011, pp. 1721-1734
[11] J.W. Wiskin, D.T. Borup, E. Iuanow, J. Klock, and M.W. Lenox, "3-D nonlinear acoustic inverse scattering: algorithm and quantitative results," IEEE Trans Ult Ferr Freq Cont, 64(8), 2017, pp. 1161-1174
[12] G.Y. Sandhu, C. Li, O. Roy, S. Schmidt, and N. Duric, "Frequency domain ultrasound waveform tomography: breast imaging using a ring transducer " Phys Med Biol, 60, 2015, pp. 5381-5398
[13] U. Vyas and D. Christensen, "Ultrasound beam simulations in inhomogeneous tissue geometries using the hybrid angular spectrum method " IEEE Trans Ult Ferr Freq Cont, 59(6), 2012, pp. 1093-1100
[14] J. Wiskin, S.A. Johnson, and M. Berggren, "Non-linear inverse scattering: high resolution quantitative breast tissue tomography," J Acoust Soc Am, 131(5), 2012, pp. 3802-3813